

k -Barrier Coverage for Physical Security in Stealthy Lattice Wireless Sensor Networks

Habib M. Ammari

Wireless Sensor and Mobile Ad-hoc Networks (WiSeMAN) Research Lab
Department of Computer and Information Science
Fordham University, Bronx, New York 10458, USA
hammari@fordham.edu

Abstract

Any unauthorized access to a critical space is a physical breach in our society that can be viewed as a physical security problem. It is essential to build a barrier that prevents any intruder's attempt to cross it and access a critical area. In this paper, we address the problem of physical security in stealthy lattice wireless sensor networks using a belt of sensors around a critical area. Precisely, we propose a theoretical framework to analyze the k -barrier coverage problem, where any path that crosses this belt intersects with the sensing range of at least k sensors, $k \geq 1$. Specifically, we analyze the k -barrier coverage problem from a tiling perspective, where the sensors' sensing disks are tangential to each other. We study two deterministic sensor deployment strategies, which yield square lattice and hexagonal lattice wireless sensor networks, respectively. First, we introduce the concept of intruder's abstract paths along a k -barrier covered sensor belt region, and compute their number. Second, we propose a polynomial representation of all abstract paths. Third, we compute the number of sensors deployed over a k -barrier covered sensor belt region for both lattices. Fourth, we define the concept of weakly k -barrier covered path crossing a k -barrier covered sensor belt region, and compute its length for both lattices. Also, we define the observability of intruder's abstract path, and compute its value for both lattices. Fifth, we provide more generalized results when the intruder moves randomly across a k -barrier covered sensor belt region. Sixth, we corroborate our analysis with simulation results.

Categories and Subject Descriptors: Network Architecture and Design; Network Protocols; Distributed Systems.

Keywords: Wireless sensor networks, physical security, k -barrier coverage, square lattice, hexagonal lattice.

1 Introduction

Physical security is an essential component for the safety and/or proper operation of several critical environments. Indeed, any unauthorized access to a critical space is a fundamental physical breach, which can be classified as a physical security problem. For instance, when people are not in their labs or offices, their equipment may be stolen and, thus, is vulnerable to theft and damage. This leads to physical security of facilities/equipment that needs to cope with. A physical security problem may yield a cybersecurity issue, where the information may be in danger.

The main goal of physical security is to detect and prevent any intrusion. Various solutions have been proposed to the physical security problem. Moats were used from the earliest medieval times as a defensive strategy against invasions. In general, the most traditional ways

to protect a facility are physical and include guards, barricades, and fences. Unfortunately, all of these safeguards provide only one layer of physical security. However, physical security is not just a barb wire fence that should be placed around a facility. Nowadays, video surveillance systems, which have a detection capability, is a key technology that could be used to track any unauthorized access to a protected area. In this paper, we propose to use lattice wireless sensor networks (WSNs), which can be viewed as a layered protection system that consists of several layers of protection, each of which has several sensors. Our philosophy is motivated by the fact that when an intruder traverses one layer of sensors, there is another layer to further detect and prevent such an intrusion activity. Given that there are multiple layers, the likelihood of an intruder being caught is high, thus, avoiding any malicious acts. In practice, it is almost impossible for an intruder to penetrate all layers without being detected. The number of layers, denoted by k , represents the strength of the physical security provided. That is, the higher value of k is, the stronger the physical security of the system is.

Our study focuses on the protection of the perimeter of a facility, such as an international border. Thus, it is essential to build a barrier that prevents any intruder's attempt to cross it and access a critical area. In this paper, we address the problem of physical security in stealthy lattice WSNs through the use of a belt of sensors (*i.e.*, barrier) surrounding a critical area. Specifically, we propose a theoretical framework to analyze the problem of k -barrier coverage, where every path crossing this belt of sensors intersects with the sensing range of at least k sensors, where $k \geq 1$. That is, a path is k -barrier covered if some (*i.e.*, at least one) or all of its points are covered by at least k sensors, which are deployed in a barrier, *i.e.*, those path points intersect with at least k sensors. Precisely, we analyze the k -barrier coverage problem from a tiling perspective, where the sensors' sensing disks are simply tangential to each other.

1.1 Problem Statement

The fundamental questions that we want to address in this paper to solve the physical security problem, can be stated as follows:

- **Question 1:** How can the sensors be deterministically placed in a belt so that every crossing path of this belt is k -barrier covered, *i.e.*, every path intersects with at least k sensors?
- **Question 2:** What is the minimum number of sensors to achieve k -barrier coverage of a belt?
- **Question 3:** What is the ratio of the communication range to the sensing range of the sensors so a belt is k -barrier covered?
- **Question 4:** What is the number of possible (or abstract) paths of an intruder crossing a k -barrier covered sensor belt? How can these abstract paths be represented?
- **Question 5:** What is the minimum size of the intersection set among all possible intersection sets between an intruder's abstract path and k -barrier covered sensor belt?

1.2 Major Contributions

Our major contributions in this paper can be stated as follows:

- We analyze the k -barrier coverage problem from a tiling perspective, where the sensors' sensing disks are kissing each other. We suggest to deploy deterministically a belt of sensors surrounding a critical area yielding a square or hexagonal lattice. In each lattice, any path crossing this belt is k -barrier covered, *i.e.*, intersects with at least k sensors. We prove that these lattices are not isomorphic. In fact, we show that a hexagonal lattice-based sensor deployment is denser than its counterpart using square lattice.
- We compute the number of sensors required to achieve k -barrier coverage of a sensor belt for each lattice.
- We determine the relationship between the communication range and sensing range of the sensors for each lattice so that a belt is k -barrier covered.
- We introduce the concept of intruder's abstract path as a sequence of k progressive moves, including left-oblique, right-oblique, and vertical line-segments only. Then, we compute the number of these paths crossing a k -barrier covered sensor belt as a function of k . Also, we provide a polynomial representation of all intruder's abstract paths.
- We introduce the concept of intruder's abstract path observability as the minimum cardinality of the intersection set among all possible intersection sets between an intruder's abstract path and a k -barrier covered sensor belt. We compute its value for each lattice.
- We generalize the above results to random intruder's motion across a k -barrier covered sensor belt. We redefine an abstract path as a sequence of left-horizontal, right-horizontal, left-oblique, right-oblique, and/or vertical line-segments.
- We corroborate our analysis with simulation results.

The remainder of this paper is structured as follows. In Section 2, we define a few key terms, and state the assumptions made to study the k -barrier coverage problem in WSNs. In Section 3, we review existing related approaches. In Section 4, we discuss the k -barrier coverage problem for two deterministic sensor deployment strategies yielding square and hexagonal lattice WSNs. In Section 5, we generalize the above discussion to account for random movement of intruders. In Section 6, we provide simulation results of our proposed study. In Section 7, we conclude and present our future work.

2 Preliminaries

In this section, we give key definitions that are essential in our study of the physical security problem in wireless sensor networks. Then, we present the main assumptions for this study.

2.1 Terminology

Definition 1 (Square and Hexagonal Lattice Wireless Sensor Networks): A *square lattice WSN* is a WSN whose sensors are deployed according to a square lattice (see Figure 1). A *hexagonal lattice WSN* is a WSN whose sensors are deployed using a hexagonal lattice (see Figure 1). ■

Definition 2 (Sensor Belt Region): A *sensor belt region* is a belt region that has a set of sensors deployed in it. ■

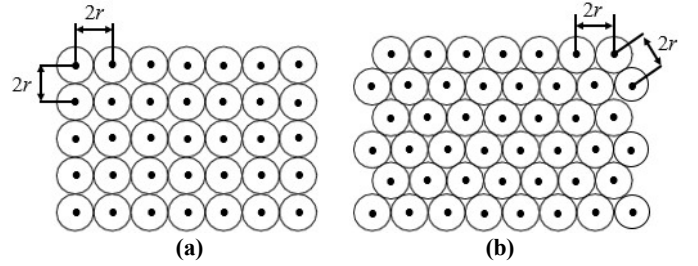


Figure 1. (a) Square lattice and (b) Hexagonal lattice (right)

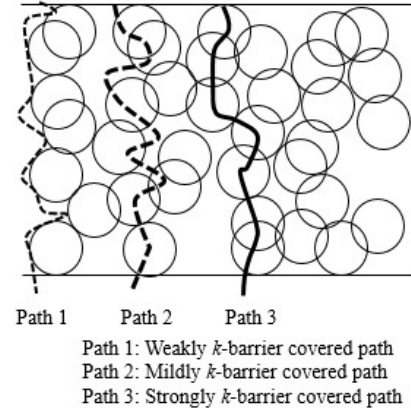


Figure 2. Weakly, mildly, strongly k -barrier covered paths

Definition 3 (Barrier): A *barrier* is an obstacle (or fence) that prevents any movement from an accessible area to an inaccessible (critical or protected) area, such as a border. ■

From Definitions 2 and 3, it is clear that a sensor belt region defines a barrier. The latter will prevent any intruder's attempt to cross it and access a critical area.

Definition 4 (k -Barrier Covered Path): A path is said to be *k -barrier covered* if it intersects with the sensing range of at least k sensors, which are deployed in a barrier, where $k \geq 1$. ■

It is worth noting that the concept of k -barrier coverage is different from that of k -coverage [1]. A path is k -covered if every point along this path is covered by at least k sensors. However, From Definition 4, a path is k -barrier covered if some or all of its points are covered by at least k sensors deployed in a barrier.

Definition 5 (Weakly, Strongly, and Mildly k -Barrier Covered Paths): Let k be a natural number, where $k \geq 1$. A *weakly k -barrier covered path* is a k -barrier covered path whose $O(k)$ of its points intersect with the sensing range of at least k sensors deployed in a barrier (Figure 2). A *strongly k -barrier covered path* is a k -barrier covered path such that each of its points intersects with the sensing range of at least one sensor among k sensors deployed in a barrier (Figure 2). A *mildly k -barrier covered path* is a k -barrier covered path that is neither weakly k -barrier covered nor strongly k -barrier covered (Figure 2). ■

Definition 6 (k -Barrier Covered Sensor Belt Region): A sensor belt region $SBR_{w,l}$ of width w and length l , is *k -barrier covered* if any path crossing its entire width w is k -barrier covered. ■

Definition 7 (Stealthy Sensor): A sensor is said to be *stealthy* if no intruder is aware of its geographic location. ■

Definition 8 (Progressive Move): An intruder's planar move from location (x_i, y_i) to location (x_j, y_j) , denoted by $(x_i, y_i) \downarrow (x_j, y_j)$, is said to be *progressive* if $y_j < y_i$. ■

2.2 Network Model

Assumption 1 (Sensor Homogeneity): All the deployed sensors are *homogeneous*, i.e., they have the same sensing range and same communication range. ■

Assumption 2 (Sensor Location Awareness): All the deployed sensors are aware of their geographic locations using a global positioning system or a localization technique [7]. ■

Assumption 3 (Sensing Disk Model): The sensing range of any deployed sensor s is represented by a disk of radius r . ■

Assumption 4 (Communication Disk Model): The communication range of any deployed sensor s is represented by a disk of radius R . ■

Assumption 5 (Belt Region and Sensor Deployment): All the sensors are *deterministically* deployed in a *rectangular belt region* of width w and length l , using square lattice based sensor deployment approach (see Figure 1) or hexagonal lattice-based sensor deployment approach (see Figure 1), where $k \geq 1$ and r stands for the radius of the sensing disk of the sensors. ■

Assumption 6 (Stealthy Sensors): All the deployed sensors in a belt region are *stealthy*. ■

Assumption 7 (Intruder Detection): Any intruder moving along a k -barrier covered path when walking through a belt region to cross a border or access a protected area, will surely be detected by at least k sensors, where $k \geq 1$ is a natural number. ■

3 Related Work

In this section, we describe a sample of approaches that dealt with the barrier coverage problem in WSNs.

In [7], Kumar *et al.* proposed the first study of the k -barrier coverage problem in WSNs. First, they investigated the weak barrier-coverage with high probability, where all intruders are guaranteed to be detected when crossing a barrier of stealthy sensors. Then, they discussed the strong barrier-coverage with high probability, which ensures the detection of all intruders when crossing a barrier of non-stealthy sensors. In [8], Liu *et al.* presented an efficient distributed algorithm for the construction of sensor barriers on long strip areas of irregular shape. Also, they presented results related to intruder detection depending on the relationship between the width and length of a rectangular area. In [15], Yang and Qiao focused on the barrier information coverage problem, which aims at reducing the number of active sensors to cover a barrier through exploiting collaborations and information fusion among neighboring sensors. In [2], Chen *et al.* introduced the concept of local barrier coverage, which allows sensors to locally determine whether a given sensor deployment can provide global barrier coverage, where all movements with trajectory confined to a slice of the belt of region of deployment are guaranteed to be detected. In [12], Saipulla *et al.* considered the problem of using mobile sensors with limited mobility to efficiently improve barrier coverage. They provided a sensor mobility scheme that maximizes the number of barriers with minimum sensor moving distances. In [16], Yang *et al.* studied the minimum-energy cost k -barrier coverage problem in WSNs, where each sensor has several sensing power levels. They modeled this problem as a minimum cost flow problem, and used Lagrangian relaxation technique to solve it. In [14], Wang *et al.*

focused on the problem of efficient use of mobile sensors to achieve k -barrier coverage. First, given a number of deployed stationary sensors, they determined the number of mobile sensors that are required to form k -barrier coverage. Then, given the deployment of stationary and mobile sensors, they computed the maximum number of formed barriers. In [4], He *et al.* investigated the barrier coverage problem in WSNs for line-based and curve-based sensor deployment. They identified the characteristics for optimal curve-based deployment. In [11], Saipulla *et al.* studied the barrier coverage of a line-based sensor deployment and used mobile sensors to improve barrier coverage. They devised an efficient algorithm for mobile sensor relocation on the deployed line to improve barrier coverage by filling gaps and balancing energy consumption among mobile sensors. In [3], He *et al.* generalized their previous work [4] to take into consideration a heterogeneous sensing model. In [5], Kim *et al.* proposed three remedies for the scheduling algorithms developed by Kumar *et al.* [9], which achieved optimal lifetime via the identification of a collection of disjoint subsets of sensors, each of which provide barrier-coverage over the area. In [6], Kim *et al.* proposed four approaches for constructing reinforced barriers, which sense any intruder movement and detect any penetration. For more details on various coverage problems in WSNs, the reader is referred to a comprehensive survey [13].

4 Tiling-Based k -Barrier Coverage

In this section, we analyze the k -barrier coverage problem from a tiling perspective. In other words, we tile a sensor belt region so it is k -barrier covered, while there is no overlap between the sensors' sensing disks. We consider two deterministic sensor deployment strategies, which yield square (Subsections 4.3) and hexagonal (Subsections 4.4) lattice WSNs, respectively.

4.1 Intruder's Abstract Path Counting

First, we define the concept of structural k -node line. Then, we present some theoretical results for its number and height.

Definition 9 (Structural k -Node Line): A *structural k -node line*, denoted by l_k , with $k \geq 1$, is a line that has k nodes such that no two of them are located at the same level. Also, each node, except the leaf node, has one left node, right node, or vertical node (for square lattice WSNs only). ■

Figure 3 shows a sample of structural k -node lines. Theorem 1 below computes the number of structural k -node lines for square lattice WSNs.

Theorem 1 (k -Node Lines Number for Square Lattice WSNs): The number of structural k -node lines for square lattice WSNs is 3^{k-1} , where $k \geq 1$ is a natural number.

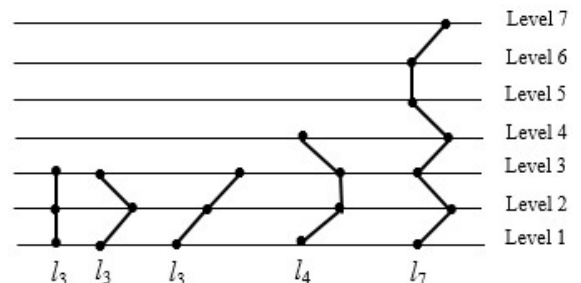


Figure 3. Sample of structural 3-node, 4-node, 7-node lines

Proof: We can proceed using a proof by mathematical induction on k . Let $P(k)$ be the following statement:

$P(k)$: “There are 3^{k-1} different structural k -node lines, where $k \geq 1$ is a natural number.”

Basis step: Let us prove that $P(k)$ is true for $k = 1$. This is trivial. In fact, there is only one structural 1-node line ($3^0 = 1$).

Inductive step: We assume that $P(m)$ is true, *i.e.*, there are 3^{m-1} different structural m -node lines, where $m \geq 1$. We want to prove that $P(m+1)$ is true. That is, the number of structural $(m+1)$ -node lines is 3^m . We start from those 3^{m-1} different structural m -node lines, and add the $(m+1)^{th}$ node to each one of them. Let q be the only leaf node of each of these structural m -node lines. There are three possibilities to add that $(m+1)^{th}$ node to each of these structural m -node lines so as to produce structural $(m+1)$ -node lines. In fact, the newly added $(m+1)^{th}$ node can be a left child, direct child, or right child of q . Therefore, the total number of produced structural $(m+1)$ -node lines is $3 \times 3^{m-1} = 3^m$, thus, proving $P(m+1)$ is true. Thus, the statement $P(k)$ is true, for all $k \geq 1$. Indeed, we have the inference rule:

$(P(1) \wedge (\forall m \geq 1, P(m) \rightarrow P(m+1))) \rightarrow P(k), \forall k \geq 1$ ■

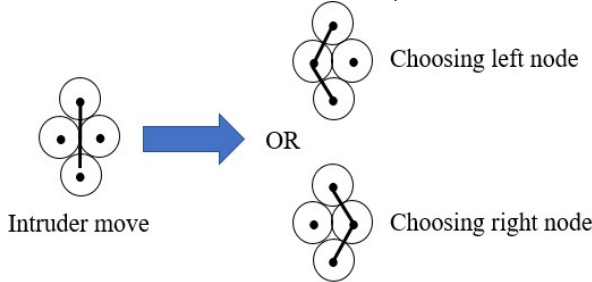


Figure 4. Crossing intersection point of two kissing sensing disks

Notice that for hexagonal lattice WSNs, any node, except the leaf node, has only one left node or one right node. That is, there is no vertical node. Indeed, there is one special case when an intruder moves from the sensing disk of a sensor node to another area through the intersection point of two kissing sensing disks of two neighboring sensors. In this situation, we choose one of these two nodes (*i.e.*, either left node or right node). Figure 4 illustrates this special case.

Theorem 2 computes the number of structural k -node lines for hexagonal lattice WSNs.

Theorem 2 (k-Node Lines Number for Hexagonal Lattice WSNs): The number of structural k -node lines for hexagonal lattice WSNs is 2^{k-1} , where $k \geq 1$ is a natural number.

Proof: Same proof method as the one for Theorem 1, except that a node can have only one left child or right child (*i.e.*, there is no direct child). ■

Lemma 1 calculates the height of a structural k -node line.

Lemma 1 (Structural k-Node Line Height): The height of a structural k -node line is $k - 1$, where $k \geq 1$.

Proof: It is easy to show this result using a mathematical induction proof on k . Let $Q(k)$ be the following statement:

$Q(k)$: “A structural k -node line has a height equal to $k - 1$, where $k \geq 1$ ”

Basis step: Let us prove that $Q(k)$ is true for $k = 1$. This structural 1-node line has height equal to 0. Thus, $Q(1)$ is true.

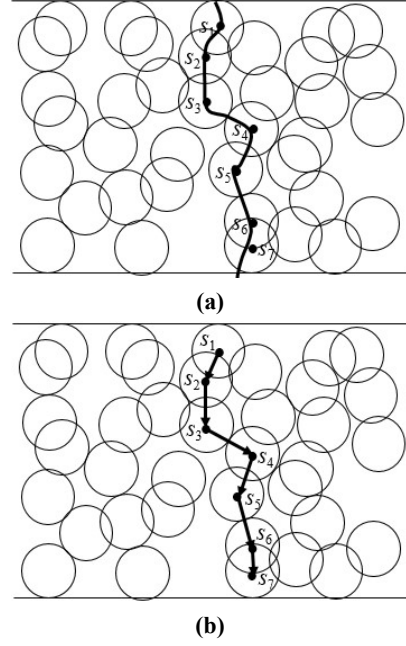


Figure 5. (a) Intruder's movement trajectory – (b) Abstract path

Inductive step: We assume that $P(m)$ is true, *i.e.*, the height of structural m -node line is $m - 1$, where $m \geq 1$. We want to prove that $Q(m+1)$ is true. That is, the height of a structural $(m+1)$ -node line is m . We add the $(m+1)^{th}$ node to a structural m -node line whose height is $m - 1$, and attach it to its leaf node as left, vertical, or right child. We obtain a structural $(m+1)$ -node line whose height is equal to that of the structural m -node line augmented by 1, *i.e.*, $(m - 1) + 1 = m$. Thus, $Q(m+1)$ is true. We have the following inference rule, which proves that $Q(k)$ is true for any $k \geq 1$.

$(Q(1) \wedge (\forall m \geq 1, Q(m) \rightarrow Q(m+1))) \rightarrow Q(k), \forall k \geq 1$ ■

Assumption 8 (Fast Sensor Belt Region Crossing): An intruder attempts to cross a sensor belt region using a shortest path. ■

Intuitively, an intruder always aims at crossing a sensor belt region (or barrier) as fast as possible so they can have access to a protected area without being detected. Hence, their movement trajectory is a sequence of *progressive* moves (or line-segments), where each line-segment is left-oblique, right-oblique, or vertical (*i.e.*, orthogonal to the sensor belt region). That is, an intruder would not make any horizontal move along a sensor belt region, thus, eliminating horizontal line-segment from their movement trajectory. Thus, an intruder's path can be viewed as a random sequence of left-oblique, right-oblique, and vertical line-segments. Given that all the sensing disks are tangential to each other for both square and hexagonal lattices, the movement trajectory of an intruder can be considered as a sequence of transitions from one sensing disk to another. In other words, all the intruder's movement trajectory, which allow them to move from the sensing disk of one sensor to that of another sensor, can be abstracted (or summarized) by only one left-oblique, right-oblique, or vertical line-segment. This depends on whether this move is from one sensing disk to another one located at its left, right, or below it, as shown in Figure 5. That is, an intruder's path can be represented by an *abstract path*, denoted by $IAP = (N, E)$, where the node set N represents the set of sensing disks,

and the edge set E stands for transitions between the sensors' sensing disks. Moreover, any intruder's abstract path has exactly k nodes and $k - 1$ edges, *i.e.*, $|N| = k$ and $|E| = k - 1$. Consequently, we conclude that the number of intruder's abstract paths along a k -barrier covered sensor belt region $SBR_{w,l}$ corresponds to the number of structural k -node lines as computed in Theorems 1 and 2. Corollary 1 below states this result.

Example: As shown in Figure 5, the intruder's abstract path corresponding to their movement trajectory and denoted by $IAP = (N, E)$ can be defined by the following two sets:

- $N = \{s_1, s_2, s_3, s_4, s_5, s_6, s_7\}$
- $E = \{(s_1, s_2), (s_2, s_3), (s_3, s_4), (s_4, s_5), (s_5, s_6), (s_6, s_7)\}$

where the first node is s_1 and last node is s_7 , from top to bottom.

Corollary 1 (Intruder's Abstract Path Cardinality): The total number of intruder's abstract paths with k vertices and $k - 1$ edges along a k -barrier covered sensor belt region is 3^{k-1} for square lattice, and 2^{k-1} for hexagonal lattice, where $k \geq 1$. ■

Table 1. All intruder's abstract paths for square lattice WSNs

	$k = 2$	$k = 3$
1 st path family	↓	↓↓
2 nd path family	↙	↙↘↘↘
3 rd path family	↘	↘↘↘↘

Table 2. All intruder's abstract paths for hexagonal lattice WSNs

	$k = 2$	$k = 3$
1 st path family	↙	↙↘
2 nd path family	↘	↘↙

Although the number of paths crossing a sensor belt region is infinite, those paths can be represented by those 3^{k-1} and 2^{k-1} intruder's abstract paths for square lattice WSNs and hexagonal lattice WSNs, respectively. That is, for square lattice WSNs, all the possible intruder's paths to cross the sensor belt region can be classified into 3^{k-1} abstract paths. Notice that those 3^{k-1} intruder's abstract paths can be classified into three families. The first family has only one path, which consists of only vertical line-segments, whereas the second and third ones have the same number of abstract paths. Moreover, the abstract paths in the second family are symmetric to their counterparts in the third one. Table 1 shows those abstract paths in the three families for $k = 2$ and $k = 3$. However, for hexagonal lattice WSNs, those 2^{k-1} intruder's abstract paths can be classified into two families, which have the same number of abstract paths. Furthermore, those paths are symmetric to each other. Table 2 shows those abstract paths in those families for $k = 2$ and $k = 3$. Next, we define the concept of intruder's abstract path observability.

Definition 10 (Intruder's Abstract Path Observability): The *observability* of an intruder's abstract path IAP along a sensor belt region $SBR_{w,l}$, denoted by O_{IAP} , is defined as the minimum

cardinality of the intersection set among all possible intersection sets between an intruder's abstract path IAP_i and $SBR_{w,l}$. Formally, O_{IAP} is computed as follows:

$$O_{IAP} = \min\{|IAP_i \cap SBR_{w,l}| | IAP_i \in IAP\}$$

where IAP is the set of all intruder's abstract paths. ■

Intuitively, the observability of an intruder's abstract path IAP measures the percentage of IAP being observed (or sensed) by those sensors that are able to detect the intruder. Notice that O_{IAP} reaches its maximum value 1 for a strongly k -barrier covered path whose all of its points intersect with the sensing disks of the sensors, and its minimum value ε_k for a weakly k -barrier covered path, which intersect with exactly k points of the sensing disks of the sensors. That is, $\varepsilon_k \leq O_{IAP} \leq 1$.

4.2 Intruder's Abstract Path Analysis

As stated earlier, there are three types of line-segments in an intruder's abstract path, namely left-oblique, right-oblique, and vertical line-segments. Let x_{LO} , x_{RO} , and x_V be three variables denoting those three types of line-segments, respectively.

Theorem 3 provides a polynomial representation of all intruder's abstract paths for square lattice WSNs.

Theorem 3 (Intruder's Abstract Path Representation for Square Lattice WSNs): All the 3^{k-1} possible intruder's abstract paths that have exactly k vertices and $(k - 1)$ edges can be represented by the following polynomial:

$$\begin{aligned} & (x_{LO} + x_{RO} + x_V)^{k-1} \\ &= \sum_{k_{LO} + k_{RO} + k_V = k-1} \binom{k-1}{k_{LO}, k_{RO}, k_V} x_{LO}^{k_{LO}} x_{RO}^{k_{RO}} x_V^{k_V} \\ & \binom{k-1}{k_{LO}, k_{RO}, k_V} = \frac{(k-1)!}{k_{LO}! k_{RO}! k_V!} \end{aligned}$$

where $k \geq 1$ is a natural number, $x_{LO}^{k_{LO}} x_{RO}^{k_{RO}} x_V^{k_V}$ is an intruder's abstract path that has k_{LO} left-oblique, k_{RO} right-oblique, and k_V vertical line-segments, and $\binom{k-1}{k_{LO}, k_{RO}, k_V}$ is the corresponding total number of such a path.

Proof: As per Lemma 1, any intruder's abstract path has a height equal to $k - 1$. That is, it has exactly $(k - 1)$ levels. Each level contains exactly one type of line-segment, *i.e.*, left-oblique, right-oblique, or vertical. Let us assimilate a level to a box, and left-oblique (type 1), right-oblique (type 2), and vertical (type 3) line-segments to three different types of objects. Therefore, we have $(k - 1)$ boxes and three types of objects. Precisely, we have $(k - 1)$ objects of each type, and each of those $k - 1$ boxes can hold exactly one instance of any type of object. We can select k_{LO} objects of type 1, k_{RO} objects of type 2, and k_V objects of type 3 such that $0 \leq k_{LO}, k_{RO}, k_V \leq k - 1$ and $k_{LO} + k_{RO} + k_V = k - 1$. Basically, we are counting the number of possible permutations of $(k - 1)$ objects subject to the above two conditions. The multinomial coefficient $\binom{k-1}{k_{LO}, k_{RO}, k_V}$ computes the number of distinct ways to permute a multiset of $(k - 1)$ objects. We used the term "multiset" because we allow the use of the same object many times. The factor $x_{LO}^{k_{LO}} x_{RO}^{k_{RO}} x_V^{k_V}$ correspond to a given multiset with k_{LO} objects of type 1, k_{RO} objects of type 2, and k_V objects of

type 3. Thus, a permutation of a multiset corresponds to an intruder's abstract path, and $\binom{k-1}{k_{LO}, k_{RO}, k_V}$ computes all possible permutation of a given multiset, thus, generating all possible intruder's abstract paths having exactly k_{LO} left-oblique, k_{RO} right-oblique, and k_V vertical line-segments. The summation symbol is used to account for all possible permutations of all possible multisets, thus, producing all possible intruder's abstract paths by varying the variables k_{LO} , k_V , and k_{RO} , subject to the following conditions:
 $0 \leq k_{LO}, k_{RO}, k_V \leq k-1$ and $k_{LO} + k_{RO} + k_V = k-1$. ■

Table 3 below shows a few examples of the above results for various values of k . For instance, for $k=1$, the intruder's abstract path is reduced to one node. For $k=2$, there are three (*i. e.*, 3^{2-1}) intruder's abstract paths, each of which has only one edge that could be left-oblique, right-oblique, or vertical. For $k=3$, there are nine (*i. e.*, 3^{3-1}) intruder's abstract paths. For instance, the first path (x_{LO}^2) has only two left-oblique line-segments, the second path (x_{RO}^2) has two right-oblique line-segments, and the third path (x_V^2) has two vertical line-segments. Also, there are two paths ($2 \times x_{LO} \times x_{RO}$), each of which has one left-oblique and one right-oblique line-segments; two paths ($2 \times x_{LO} \times x_V$), each of which has one left-oblique and one vertical line-segments; and two paths ($2 \times x_{RO} \times x_V$), each of which has one right-oblique and one vertical line-segments. We use the same interpretation for $k=4$.

Table 3. Polynomial representation of all intruder's abstract paths

k	$(x_{LO} + x_{RO} + x_V)^{k-1}$
1	1
2	$x_{LO} + x_{RO} + x_V$
3	$x_{LO}^2 + x_{RO}^2 + x_V^2 + 2 \times x_{LO} \times x_{RO} + 2 \times x_{LO} \times x_V + 2 \times x_{RO} \times x_V$
4	$x_{LO}^3 + x_{RO}^3 + x_V^3 + 3x_{LO}^2x_{RO} + 3x_{LO}^2x_V + 3x_{LO}x_{RO}^2 + 3x_{LO}x_V^2 + 3x_{RO}^2x_V + 3x_{RO}x_V^2 + 6x_{LO}x_{RO}x_V$

Theorem 4 gives a polynomial representation of all intruder's abstract paths for hexagonal lattice WSNs.

Theorem 4 (Intruder's Abstract Path Representation for Hexagonal Lattice WSNs): All the 2^{k-1} possible intruder's abstract paths that have exactly k vertices and $(k-1)$ edges can be represented by the following polynomial:

$$(x_{LO} + x_{RO})^{k-1} = \sum_{k_{LO}+k_{RO}+k_V=k-1} \binom{k-1}{k_{LO}, k_{RO}} x_{LO}^{k_{LO}} x_{RO}^{k_{RO}}$$

$$\binom{k-1}{k_{LO}, k_{RO}} = \frac{(k-1)!}{k_{LO}! k_{RO}!}$$

where $k \geq 1$, $x_{LO}^{k_{LO}} x_{RO}^{k_{RO}}$ is an intruder's abstract path that has k_{LO} left-oblique and k_{RO} right-oblique line-segments, and $\binom{k-1}{k_{LO}, k_{RO}}$ is the corresponding total number of such a path.

Proof: We follow the same proof as the one for Theorem 3. But, there is no vertical line-segment. ■

Let $\Omega_{IAP}^{SL}(k_{LO}, k_{RO}, k_V, k)$ denote the total number of possible intruder's abstract paths $x_{LO}^{k_{LO}} x_{RO}^{k_{RO}} x_V^{k_V}$ for square lattice WSNs, each of which contains k_{LO} left-oblique line-segments, k_{LO} right-oblique line-segments, and k_V vertical line-segments, where $0 \leq k_{LO}, k_{RO}, k_V \leq k-1$ and $k_{LO} + k_{RO} + k_V = k-1$. From Theorem 3 above, we have the following equality:

$$\Omega_{IAP}^{SL}(k_{LO}, k_{RO}, k_V, k) = \sum_{k_{LO}+k_{RO}+k_V=k-1} \binom{k-1}{k_{LO}, k_{RO}, k_V}$$

$$= \sum_{k_{LO}+k_{RO}+k_V=k-1} \frac{(k-1)!}{k_{LO}! k_{RO}! k_V!}$$

From Theorem 4, the total number $\Omega_{IAP}^{HL}(k_{LO}, k_{RO}, k)$ of intruder's abstract paths $x_{LO}^{k_{LO}} x_{RO}^{k_{RO}}$ for hexagonal lattice WSNs, each of which contains k_{LO} left-oblique line-segments and k_{RO} right-oblique line-segments, where $0 \leq k_{LO}, k_{RO} \leq k-1$ and $k_{LO} + k_{RO} = k-1$, is computed as follows:

$$\Omega_{IAP}^{HL}(k_{LO}, k_{RO}, k) = \sum_{k_{LO}+k_{RO}=k-1} \binom{k-1}{k_{LO}, k_{RO}}$$

$$= \sum_{k_{LO}+k_{RO}=k-1} \frac{(k-1)!}{k_{LO}! k_{RO}!}$$

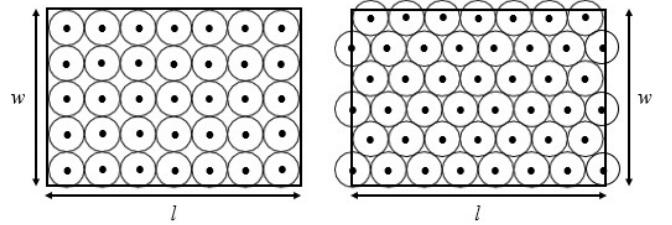


Figure 6. k -barrier covered sensor belt region $SBR_{w,l}$ for square (left) and hexagonal (right) sensor deployment

There are two optimal deterministic sensor deployment approaches in a 2D field, namely square and hexagonal lattice-based sensor deployment, over a k -barrier covered sensor belt region $SBR_{w,l}$, with w being its width, and l its length. Indeed, there are two types of lattice patterns in the literature, namely square lattice and hexagonal lattice. As per Assumption 5, the sensors are deployed according to each of these two sensor deployment strategies. Figure 6 shows the configuration for each of these two types of lattice patterns. Next, we study the k -barrier coverage problem in both lattices.

4.3 Square Lattice-Based Sensor Deployment

Consider a row of sensors in a square lattice. Notice that the difference between the x -coordinates of the centers of two adjacent sensors is $2r$. That is, the x -coordinate increases by $2r$, while the y -coordinate remains the same as we move from one sensor to another in the same row. Likewise, the difference between the y -coordinates of the centers of two adjacent sensors located on the column is $2r$. In other words, the y -coordinate increases by $2r$, while the x -coordinate does not change as we move from one sensor to another in the same column.

Theorem 5 computes the total number of deployed sensors to achieve k -barrier coverage in square lattice WSNs.

Theorem 5 (Sensor Cardinality for Square Lattice Deployment): The number of sensors deployed over a k -barrier covered sensor belt region $SBR_{w,l}$ according to a square lattice-based sensor deployment, denoted by n_{SL} , is computed as

$$n_{SL} = \alpha k$$

where $k \geq 1$ is a natural number, $\alpha = \lceil l/2r \rceil$, and $k = \lceil w/2r \rceil$.

Proof: Assume that the sensors are deployed over a k -barrier covered sensor belt region $SBR_{w,l}$ according to a square lattice-based sensor deployment. Given that $SBR_{w,l}$ has a width w and a length l , there are $k = \lceil w/2r \rceil$ rows of sensors, each of which has $\alpha = \lceil l/2r \rceil$ sensors (*i.e.*, α is the number of columns). Therefore, the total number of sensors deployed over $SBR_{w,l}$ is $n_{SL} = \lceil w/2r \rceil \lceil l/2r \rceil$, where $k \geq 1$. ■

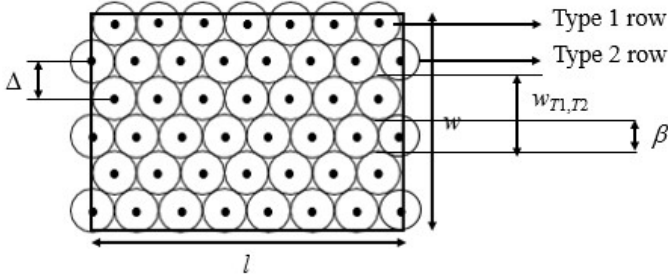


Figure 7. Difference Δ , and type 1 and type 2 rows

As stated in Theorem 5 above, there are $\lceil w/2r \rceil$ rows and $\lceil l/2r \rceil$ columns of sensors in a square lattice. A more detailed description of the locations of the sensors is given below.

- The first row (from bottom to top) includes sensors located at (r, r) , $(3r, r)$, $(5r, r)$, ..., $((2j + 1)r, r)$, ..., $(\lceil l/2r \rceil r, r)$
- The second row includes sensors located at $(r, 3r)$, $(3r, 3r)$, $(5r, 3r)$, ..., $((2j + 1)r, 3r)$, ..., $(\lceil l/2r \rceil r, 3r)$
- The third row includes sensors located at $(r, 5r)$, $(3r, 5r)$, $(5r, 5r)$, ..., $((2j + 1)r, 5r)$, ..., $(\lceil l/2r \rceil r, 5r)$
- The i^{th} row (from bottom to top) includes sensors located at $(r, (2i - 1)r)$, $(3r, (2i - 1)r)$, $(5r, (2i - 1)r)$, ..., $((2j + 1)r, (2i - 1)r)$, ..., $(\lceil l/2r \rceil r, (2i - 1)r)$

The last, (k^{th} or $\lceil w/2r \rceil^{th}$), row includes sensors located at locations whose x - y coordinates are $(r, (2k - 1)r)$, $(3r, (2k - 1)r)$, $(5r, (2k - 1)r)$, ..., $((2j + 1)r, (2k - 1)r)$, ..., $(\lceil l/2r \rceil r, (2k - 1)r)$

4.4 Hexagonal Lattice-Based Sensor Deployment

In this case, the difference between the x -coordinates of the centers of two adjacent sensors located in the same row is $2r$. However, the difference between the y -coordinates of the centers of two sensors located in two adjacent rows is Δ . As shown in Figure 7, the latter can be computed as follows:

$$\Delta^2 + r^2 = (2r)^2 \Rightarrow \Delta = \sqrt{3}r$$

Theorem 6 computes the total number of deployed sensors to achieve k -barrier coverage in hexagonal lattice WSNs.

Theorem 6 (Sensor Cardinality for Hexagonal Lattice Deployment): The number of sensors deployed over a k -barrier covered sensor belt region $SBR_{w,l}$ according to a hexagonal lattice-based sensor deployment, denoted by n_{HL} , is given by

$$n_{HL} = k_1 \left\lceil \frac{l}{2r} \right\rceil + k_2 \left(\left\lceil \frac{l}{2r} \right\rceil + 1 \right)$$

$$k_1 = \left\lfloor \frac{w}{2\sqrt{3}r} \right\rfloor$$

$$k_2 = \left\lfloor \frac{w}{2\sqrt{3}r} \right\rfloor$$

where $k = k_1 + k_2 \geq 1$ is a natural number.

Proof: As shown in Figure 7, k -barrier covered sensor belt region $SBR_{w,l}$ has two types of rows, namely Type 1 and Type 2. The sensors are deployed deterministically using a top-down approach. That is, we start with forming the first row of Type 1, then the second row of Type 2, then the third row of Type 1, etc. In other words, $SBR_{w,l}$ is built as an alternation of rows of Type 1 and Type 2. Let k_1 and k_2 be the numbers of rows of Type 1 and Type 2, respectively. It is clear that $k_1 \geq k_2$ since the starting row is of Type 1. More precisely, we have $k_1 = k_2$ or $k_1 = k_2 + 1$. Given that type of hexagonal tiling of $SBR_{w,l}$, any pair of consecutive rows of Type 1 and Type 2, respectively, have a width, denoted by $\omega_{T1,T2}$, which is less than twice the diameter of the sensors' sensing disk of radius $2r$ (*i.e.*, $\omega_{T1,T2} < 2 \times 2r = 4r$). Let $\omega_{T1,T2} = 2r + \beta$ as shown in Figure 7. As it can be seen, we have $\beta = 2(d_1 + d_2)$, where

$$d_1 = r \times \sin \theta = r \sin 30^\circ = \frac{r}{2}$$

Also, we have:

$$D = r \times \cos \theta = r \cos 30^\circ = \sqrt{3}r/2$$

$$d = 2r - 2D = (2 - \sqrt{3})r$$

Using Pythagorean's Theorem, we have:

$$d_2 = \sqrt{d^2 - \left(\frac{d}{2}\right)^2} = \frac{\sqrt{3}d}{2} = \left(\frac{2\sqrt{3} - 3}{2}\right)r$$

Thus, we have:

$$\beta = 2(d_1 + d_2) = (2\sqrt{3} - 2)r$$

Consequently, the width $\omega_{T1,T2} = 2r + \beta = 2\sqrt{3}r$

The numbers of sensors deployed in any row of Type 1 and Type 2 are, respectively, given by:

$$n_{T1} = \left\lfloor \frac{l}{2r} \right\rfloor$$

$$n_{T2} = \left\lfloor \frac{l}{2r} \right\rfloor + 1$$

If the width w of $SBR_{w,l}$ is a multiple of the width $\omega_{T1,T2}$ of two consecutive rows of Type 1 and type 2, respectively, *i.e.*, $w = a \times \omega_{T1,T2}$, we necessarily have $k_1 = k_2$. Otherwise, we get $k_1 = k_2 + 1$. Thus, the numbers of rows of Type 1 and Type 2, denoted by k_1 and k_2 , respectively, are computed as:

$$k_1 = \left\lfloor \frac{w}{\omega_{T1,T2}} \right\rfloor = \left\lfloor \frac{w}{2\sqrt{3}r} \right\rfloor$$

$$k_2 = \left\lfloor \frac{w}{\omega_{T1,T2}} \right\rfloor = \left\lfloor \frac{w}{2\sqrt{3}r} \right\rfloor$$

Therefore, the total number of sensors deployed over $SBR_{w,l}$ according to a hexagonal lattice-based sensor deployment, denoted by n_{HL} , is given by

$$n_{HL} = k_1 \left\lceil \frac{l}{2r} \right\rceil + k_2 \left(\left\lceil \frac{l}{2r} \right\rceil + 1 \right)$$

Consequently, there are $\lfloor w/\sqrt{3}r \rfloor$ rows in a hexagonal lattice.

- The first row (from bottom to top) includes sensors located at (r, r) , $(3r, r)$, $(5r, r)$, ..., $((2j+1)r, r)$, ..., $(\lfloor l/2r \rfloor r, r)$
- The second row includes sensors located at $(0, (\sqrt{3}+1)r)$, $(2r, (\sqrt{3}+1)r)$, $(4r, (\sqrt{3}+1)r)$, ..., $(2jr, (\sqrt{3}+1)r)$, ..., $(\lfloor l/2r \rfloor + 1)r, (\sqrt{3}+1)r)$
- The third row includes sensors located at $(r, (2\sqrt{3}+1)r)$, $(3r, (2\sqrt{3}+1)r)$, $(5r, (2\sqrt{3}+1)r)$, ..., $((2j+1)r, (2\sqrt{3}+1)r)$, ..., $(\lfloor l/2r \rfloor r, (2\sqrt{3}+1)r)$
- The fourth row includes sensors located at $(0, (3\sqrt{3}+1)r)$, $(2r, (3\sqrt{3}+1)r)$, $(4r, (3\sqrt{3}+1)r)$, ..., $(2jr, (3\sqrt{3}+1)r)$, ..., $(\lfloor l/2r \rfloor + 1)r, (3\sqrt{3}+1)r)$
- The $(2i-1)^{th}$ row (from bottom to top) includes sensors located at $(r, ((2i-2)\sqrt{3}+1)r)$, $(3r, ((2i-2)\sqrt{3}+1)r)$, $(5r, ((2i-2)\sqrt{3}+1)r)$, ..., $((2j+1)r, ((2i-2)\sqrt{3}+1)r)$, ..., $(\lfloor l/2r \rfloor r, ((2i-2)\sqrt{3}+1)r)$
- The $(2i)^{th}$ row (from bottom to top) includes sensors located at $(0, ((2i-1)\sqrt{3}+1)r)$, $(2r, ((2i-1)\sqrt{3}+1)r)$, $(4r, ((2i-1)\sqrt{3}+1)r)$, ..., $(2jr, ((2i-1)\sqrt{3}+1)r)$, ..., $(\lfloor l/2r \rfloor + 1)r, ((2i-1)\sqrt{3}+1)r)$

The sensor deployment in the last row depends on whether k is odd or even.

- *Case 1: k is odd*

The last, (k^{th} or $\lfloor w/2r \rfloor^{th}$), row includes sensors located at $(r, ((k-1)\sqrt{3}+1)r)$, $(3r, ((k-1)\sqrt{3}+1)r)$, $(5r, ((k-1)\sqrt{3}+1)r)$, ..., $((2j+1)r, ((k-1)\sqrt{3}+1)r)$, ..., $(\lfloor l/2r \rfloor r, ((k-1)\sqrt{3}+1)r)$

- *Case 2: k is even*

The k^{th} row (from bottom to top) includes sensors located at $(0, ((k-1)\sqrt{3}+1)r)$, $(2r, ((k-1)\sqrt{3}+1)r)$, $(4r, ((k-1)\sqrt{3}+1)r)$, ..., $(2jr, ((k-1)\sqrt{3}+1)r)$, ..., $(\lfloor l/2r \rfloor + 1)r, ((k-1)\sqrt{3}+1)r)$

4.5 Square Lattice vs. Hexagonal Lattice

Next, we study the k -barrier coverage problem for each of these two sensor deployment strategies.

Corollary 2 shows that square lattice and hexagonal lattice are not isomorphic.

Corollary 2 (Lattice Isomorphism): A square lattice WSN and a hexagonal lattice WSN deployed over a k -barrier covered sensor belt region $SBR_{w,l}$ are not isomorphic.

Proof: There is at least one sensor in a hexagonal lattice WSN that does not have any corresponding sensor in a square lattice WSN. In fact, the two lattice WSNs have unequal number of sensors, *i.e.*, a hexagonal WSN has more sensors than a square lattice deployed over $SBR_{w,l}$. ■

Theorem 7 shows that hexagonal lattice WSNs are denser than square lattice WSNs.

Theorem 7 (Hexagonal Lattice vs. Square Lattice-Based Sensor Deployment): A hexagonal lattice-based sensor deployment over a k -barrier covered sensor belt region $SBR_{w,l}$ is denser than its counterpart using a square lattice. We have the following relationship between n_{HL} and n_{SL} :

$$n_{HL} = \frac{1}{\sqrt{3}} \left(2 + \frac{1}{\lfloor \frac{l}{2r} \rfloor} \right) n_{SL}$$

Proof: Without loss of generality, let us assume that the numbers of rows of Type 1 (*i.e.*, k_1) and Type 2 (*i.e.*, k_2) are equal. That is, $k_1 = k_2 = \lfloor \frac{w}{2\sqrt{3}r} \rfloor$. We obtain:

$$n_{HL} = \left\lfloor \frac{w}{2\sqrt{3}r} \right\rfloor \left(2 \left\lfloor \frac{l}{2r} \right\rfloor + 1 \right)$$

Therefore, we get:

$$\frac{n_{HL}}{n_{SL}} = \frac{\left\lfloor \frac{w}{2\sqrt{3}r} \right\rfloor \left(2 \left\lfloor \frac{l}{2r} \right\rfloor + 1 \right)}{\left\lfloor \frac{w}{2r} \right\rfloor \left\lfloor \frac{l}{2r} \right\rfloor} = \frac{1}{\sqrt{3}} \left(2 + \frac{1}{\left\lfloor \frac{l}{2r} \right\rfloor} \right) \Rightarrow n_{HL} = \frac{1}{\sqrt{3}} \left(2 + \frac{1}{\left\lfloor \frac{l}{2r} \right\rfloor} \right) n_{SL} \quad \blacksquare$$

4.5.1 Voronoi Diagram-Based Comparison

It is well known that Voronoi diagram is one of the fundamental constructs that is defined by a discrete set of points. As stated in [2], the Voronoi diagram associated with a set of points in the plane divides the plane based on the nearest-neighbor rule, where every point is associated with the closest region of the plane to it. In our case, we compute the Voronoi diagram [2] of a set of points that correspond to the locations of the sensors, which are positioned according to square and hexagonal sensor deployment strategies. Figures 8 and 9 show the Voronoi diagram corresponding to a square lattice and hexagonal lattice of 100 points, respectively. All the Voronoi regions are identical for each type of lattice. A Voronoi region is a square for a square lattice, while it is a hexagon for a hexagonal lattice.

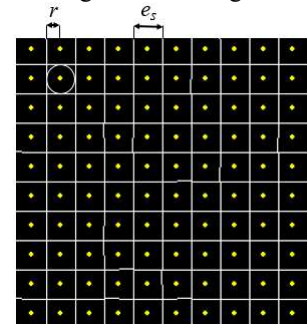


Figure 8. Voronoi diagram for a square lattice of 100 sites

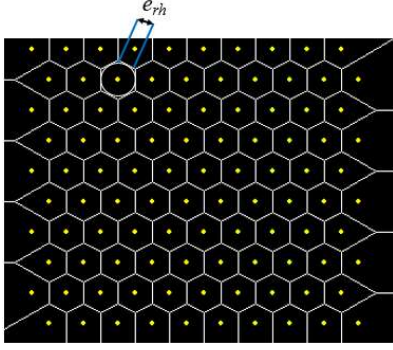


Figure 9. Voronoi diagram for a hexagonal lattice of 100 sites

In this comparison between square lattice and hexagonal lattice WSNs, our analysis focuses on their weakly k -barrier covered paths, *i.e.*, worst-case scenario for intruder detection. Hence, we want to compute the observability metric in order to compare between these two types of lattice WSNs. Indeed, observability defines the worst-case behavior of $SBR_{w,l}$ in terms of its detection capability. By definition of this geometric structure, a path from the top to the bottom through Voronoi diagram, which is as far as possible from any point, is a sequence of Voronoi edges. This path is a weakly k -barrier covered path crossing $SBR_{w,l}$. As it can be seen, there is a large number of such a path for both lattice-based sensor deployment strategies. However, for each one of them, there are a few shortest weakly k -barrier covered paths crossing $SBR_{w,l}$. For a square lattice, this path is a sequence of vertical Voronoi edges, and the length of this path is equal to the number of sites forming a column of the lattice. Each Voronoi edge has a length that is equal to the diameter of the sensors' sensing disks, *i.e.*, $2r$. However, for a hexagonal lattice, a shortest weakly k -barrier covered path consists of alternating sequence of vertical, left-oblique, and right-oblique edges.

Theorem 8 computes the length of a shortest weakly k -barrier covered path for square and hexagonal lattice WSNs.

Theorem 8 (Shortest Weakly k -Barrier Covered Path): The lengths of the shortest weakly k -barrier covered paths crossing a k -barrier covered sensor belt region $SBR_{w,l}$ are $ke_s = w$ and $4k_1e_{rh} = 4w/3$ for square lattice and hexagonal lattices, respectively, where e_s and e_{rh} are the edge lengths of the smallest square and regular hexagon, respectively, which are inscribed in a circle of radius r (*i.e.*, radius of sensing disk).

Proof: For a square lattice, a Voronoi region is a square whose edge length e_s is equal to the diameter of the sensors' sensing disks, *i.e.*, $e_s = 2r$. Indeed, this Voronoi region corresponds to the smallest square containing a disk of diameter equal to $2r$, as shown in Figure 8. For a hexagonal lattice, a Voronoi region is the smallest regular hexagon that includes a disk of diameter equal to $2r$. Figure 9 shows a disk of radius r inscribed in a regular hexagon. The edge length e_{rh} of this smallest regular hexagon can be computed as follows:

$$\tan \theta = \tan 30^\circ = \frac{1}{\sqrt{3}} = \frac{\frac{e_{rh}}{2}}{r} \Rightarrow e_{rh} = \frac{2}{\sqrt{3}}r$$

First, let us consider a square lattice WSN. In this case, a weakly k -barrier covered path crossing a k -barrier covered sensor belt region $SBR_{w,l}$ has to follow only the Voronoi edges for a square

lattice. As shown in the Voronoi diagram associated with a square lattice, the shortest weakly k -barrier covered path along $SBR_{w,l}$ has to traverse all $k = \lceil w/2r \rceil$ rows, each of which has a width equal to the edge length e_s of the smallest square including a circle of radius r . Thus, the length of this shortest path, denoted by l_{SL} , is given by:

$$l_{SL} = ke_s = \left\lceil \frac{w}{2r} \right\rceil 2r = w$$

Now, for a hexagonal lattice WSN, without loss of generality, assume that the number of rows of Type 1 is equal to that of Type 2, *i.e.*, $k_1 = k_2 = \lceil w/2\sqrt{3}r \rceil$. In this case, as it can be seen from the Voronoi diagram associated with a hexagonal lattice, the shortest weakly k -barrier covered path along $SBR_{w,l}$ includes a pair of vertical Voronoi edge from a row of Type 1 and right-oblique Voronoi edge shared between a row of Type 1 and its neighboring one of Type 2, and a pair of vertical Voronoi edge and left-oblique Voronoi edge shared between a row of Type 1 and its neighboring one of Type 2. While those vertical Voronoi edges belong alternatively to two parallel lines, the oblique Voronoi edges form an alternating sequence of right-oblique and left-oblique edges. Precisely, this path has $2k_1$ vertical, $2k_2/2$ right-oblique, and $2k_2/2$ left-oblique Voronoi edges. Thus, the length of this shortest path, denoted by l_{HL} , is computed as:

$$\begin{aligned} l_{HL} &= (2k_1 + 2k_2/2 + 2k_2/2)e_{rh} = 4k_1e_{rh} \\ &= 4 \left\lceil \frac{w}{2\sqrt{3}r} \right\rceil \frac{2}{\sqrt{3}}r = \frac{4w}{3} > w \end{aligned} \quad \blacksquare$$

Theorem 9 computes the intruder's abstract path observability for square and hexagonal lattice WSNs.

Theorem 9 (Intruder's Abstract Path Observability): The intruder's abstract path observability, denoted by O_{IAP} , along a k -barrier covered sensor belt region $SBR_{w,l}$ is equal to $\lceil w/2r \rceil$ for a square lattice WSN, and $2\lceil w/\sqrt{3}r \rceil$ for a hexagonal lattice WSN, where w is the width of $SBR_{w,l}$, and r stands for the radius of the sensors' sensing disk.

Proof: Given the definition of intruder's abstract path observability (Definition 10), we consider the weakly k -barrier covered path crossing a k -barrier covered sensor belt region $SBR_{w,l}$. That is, observability defines the worst-case behavior of $SBR_{w,l}$ in terms of its detection capability. It computes the minimum number of times an intruder would be detected as they cross $SBR_{w,l}$. Indeed, an intruder would be detected only $\Theta(k)$ times when they cross $SBR_{w,l}$ through a weakly k -barrier covered path. Because all the sensing disks are touching each other, regardless of whether we deal with a square lattice WSN or hexagonal lattice WSN, the intersection set between this weakly k -barrier covered path and $SBR_{w,l}$ coincides with the set of its vertical, left-oblique, and/or right-oblique Voronoi edges. Thus, for a square lattice, we get $O_{IAP} = k = \lceil w/2r \rceil$, and for a hexagonal lattice, we have $O_{IAP} = 2k_1 + 2k_2/2 + 2k_2/2 = 4k_1 = 4\lceil w/2\sqrt{3}r \rceil = 2\lceil w/\sqrt{3}r \rceil$. \blacksquare

4.6 Discussion

We can claim that a hexagonal lattice-based sensor deployment is better than its counterpart using square lattice over a k -barrier covered sensor belt region $SBR_{w,l}$. Indeed, a hexagonal lattice has more advantageous features compared to a square lattice.

- First, the sensing disks are distributed over $SBR_{w,l}$ more tightly for a hexagonal lattice than a square lattice, thus, allowing a better communication among the sensors. For instance, in a square lattice WSN, each sensor's sensing disks touches exactly four other sensing disks. Assuming that the radius of the sensors' communication range is twice their sensing range, *i.e.*, $R = 2r$, any sensor would be able to communicate with only four neighboring sensors although it has eight neighboring ones. Indeed, as shown in Figure 1 (a), each sensor is at distance $2r$ away from four of his eight neighboring sensors, and at distance $2\sqrt{2}r$ away from the remaining four neighboring ones. However, for a hexagonal lattice, each sensor is at distance $2r$ away from each of its six neighboring sensors, as shown in Figure 1 (b). This kind of uniformity helps the sensors in a hexagonal lattice exchange more useful data for intruder tracking compared with their counterpart in a square lattice.
- Second, the length of the weakly k -barrier covered path over $SBR_{w,l}$ for a hexagonal lattice is longer than its counterpart for a square lattice. Hence, an intruder would take more time to cross the sensor belt region $SBR_{w,l}$, thus, increasing their detection by the sensors.
- Third, the observability for a hexagonal lattice is higher than that for a square lattice. This helps increase both the quality of detection and tracking.

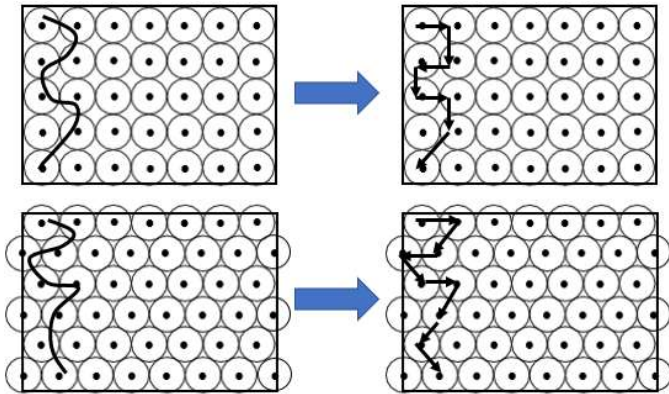


Figure 10. Intruder's movement trajectory and associated abstract path for square and hexagonal lattices

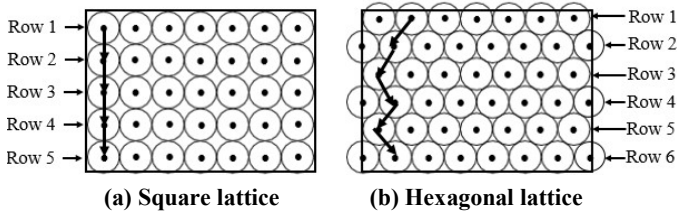


Figure 11. Shortest intruder's abstract path for both lattices

5 Generalization

Assumption 9 (Random Sensor Belt Region Crossing): An intruder moves randomly across a sensor belt region. ■

In general, an intruder may cross a sensor belt region randomly, thus, following a path including a random sequence of line-segments that are not necessarily *progressive*. Precisely, the trajectory of an intruder's movement could include moves between the sensing disks of sensors located at the same level of

the sensor belt region although those moves may be through left-oblique or right-oblique line-segments. It is worth noting that an abstract path through a hexagonal lattice does not include any vertical line-segment. Indeed, when an intruder passes vertically through the (unique) intersection point of two kissing sensing disks, we represent that intruder's move by either a left-oblique or a right-oblique line-segment. Figure 10 shows such intruder's moves and the corresponding abstract path to both square and hexagonal lattices. Consequently, an intruder's abstract path may include left-horizontal, right-horizontal, left-oblique, right-oblique, and/or vertical line-segments (this last type of line-segment is for square lattice only). Likewise, an intruder's abstract path can be modeled by a graph denoted by $IAP = (N, E)$, where the node set N represents the set of sensing disks, and the edge set E stands for transitions between the sensors' sensing disks, with $|N| \geq k$ and $|E| \geq k - 1$.

Theorem 10 (Shortest and Longest Intruder's Abstract Paths): The length of the shortest intruder's abstract path along a k -barrier covered sensor belt region SBR_w is $k - 1$. That is, it has k nodes and $(k - 1)$ edges, including only left-oblique, right-oblique, and/or vertical line-segments (for square lattice only). The length of the longest intruder's abstract path along a k -barrier covered sensor belt region $SBR_{w,l}$ is $ak - 1$. That is, it has ak nodes and $ak - 1$ edges, including exactly $(k - 1)$ vertical line-segments (for square lattice only), and $(\alpha - 1)k$ left-horizontal and right-horizontal line-segments, where $k \geq 1$ is a natural number, $w = 2kr$, and $l = 2\alpha r$.

Proof: Since the sensor belt region $SBR_{w,l}$ has k rows of sensors, there are at least $(k - 1)$ transitions between these k rows in order to cross $SBR_{w,l}$. That is, the shortest path crossing $SBR_{w,l}$ has $(k - 1)$ edges, as shown in Figure 11. Thus, the length of the shortest intruder's abstract path is $(k - 1)$. Moreover, this path does not include any left-horizontal or right-horizontal line-segments. Otherwise, it would have more than $(k - 1)$ edges. It can have only left-oblique, right-oblique, and/or vertical edges (or line-segments). Indeed, only these types of edges help the intruder to move from one row to another. The longest intruder's abstract path includes all nodes in $SBR_{w,l}$. Although all the intruder's moves are progressive, they could traverse all the sensors' sensing disks in $SBR_{w,l}$. That is, the intruder has to visit the sensing disks of all the sensors deployed in $SBR_{w,l}$. Given that each row has α nodes, there are $(\alpha - 1)$ left-horizontal or right-horizontal edges between them. Since $SBR_{w,l}$ has k rows, there are $(\alpha - 1)k$ left-horizontal and right-horizontal edges. Precisely, if k is even, the numbers of left-horizontal and right-horizontal edges, denoted by E_{LH} and E_{RH} , respectively, are the same, and are equal to $(\alpha - 1)k / 2$. If k is odd, the difference between E_{LH} and E_{RH} is $\alpha - 1$. That is, we have $|E_{LH} - E_{RH}| = \alpha - 1$. More specifically, if the starting edge of this longest path is left-horizontal, we have $E_{LH} - E_{RH} = \alpha - 1$. Otherwise (*i.e.*, the starting edge is right-horizontal), we have $E_{RH} - E_{LH} = \alpha - 1$. In the case of square lattice, for an intruder to move from one row to its next one, there is one vertical edge. For all the transitions between consecutive rows in $SBR_{w,l}$, there should be $(k - 1)$ vertical edges. In the case of hexagonal lattice, there should be $(k - 1)$ left-oblique and right-oblique edges to allow

transitions between consecutive rows in $SBR_{w,l}$. Hence, the total number of edges that are needed to cross the entire $SBR_{w,l}$ is $(\alpha - 1)k + k - 1 = \alpha k - 1$. Thus, the length of the longest intruder's abstract path is $\alpha k - 1$ in both lattices. ■

Lemma 2 states the main characteristic of all intruder's abstract paths.

Lemma 2 (Intruder's Abstract Path Characteristic): Every path across a k -barrier covered sensor belt region $SBR_{w,l}$ is characterized by the presence of $(k - 1)$ left-oblique, right-oblique, and/or vertical edges, where $k \geq 1$ is a natural number.

Proof: The only edges that enable an intruder's abstract path to cross k -barrier covered sensor belt region $SBR_{w,l}$ are left-oblique, right-oblique, and vertical edges. Given that $SBR_{w,l}$ has k rows of sensors, there are exactly $(k - 1)$ transitions between consecutive rows. Thus, any path crossing $SBR_{w,l}$ has $(k - 1)$ left-oblique, right-oblique, and/or vertical edges. ■

Theorem 11 characterizes the structure of all random intruder's abstract paths.

Theorem 11 (Random Intruder's Abstract Path Structure): Let μ_{IAP}^{Rand} be the length of a random intruder's abstract path $IAP_{Rand} = (E_{Rand}, N_{Rand})$ across a k -barrier covered sensor belt region $SBR_{w,l}$. If $\mu_{IAP}^{Rand} = k - 1$, the edge set E_{Rand} includes only left-oblique, right-oblique, and/or vertical edges. If $k \leq \mu_{IAP}^{Rand} \leq \alpha k - 1$, the edge set E_{Rand} has exactly $\mu_{IAP}^{Rand} - (k - 1)$ left-horizontal and/or right-horizontal edges, where $k \geq 1$ is a natural number, $w = 2kr$, and $l = 2\alpha r$.

Proof: From Lemma 2, if $\mu_{IAP}^{Rand} = k - 1$, all the edges should be left-oblique, right-oblique, and/or vertical. Given that we have only five types of edges (*i.e.*, left-oblique, right-oblique, vertical, left-horizontal and right-horizontal edges), if $k \leq \mu_{IAP}^{Rand} \leq \alpha k - 1$, by Lemma 2, there are exactly $(k - 1)$ left-oblique, right-oblique, and/or vertical edges, and all other $\mu_{IAP}^{Rand} - (k - 1)$ edges should be left-horizontal and/or right-horizontal. ■

Theorem 12 computes the total number of random intruder's abstract paths based on Assumption 9 and the above analysis.

Theorem 12 (Random Intruder's Abstract Path Cardinality): Let $\Omega_{IAP}^{Rand}(k_{LO}, k_{RO}, k_V, k_{LH}, k_{RH}, k)$ denote the total number of all intruder's abstract paths $x_{LO}^{k_{LO}} x_{RO}^{k_{RO}} x_V^{k_V} x_{LH}^{k_{LH}} x_{RH}^{k_{RH}}$ across a k -barrier covered sensor belt region $SBR_{w,l}$, under Assumption 9 stated earlier. Each of these paths has k_{LO} left-oblique line-segments, k_{RO} right-oblique line-segments, k_V vertical line-segments (for square lattice only), k_{LH} left-horizontal line-segments, and/or k_{RH} right-horizontal line-segments, where $0 \leq k_{LO}, k_{RO}, k_V \leq k - 1$, $k_{LO} + k_{RO} + k_V = k - 1$, $k_{LH} + k_{RH} = \mu_{IAP}^{Rand} - \mu_{IAP}^{Fast} = \mu_{IAP}^{Rand} - (k - 1)$, $k \geq 1$ is a natural number, $w = 2kr$, and $l = 2\alpha r$. We have this result:

$$\Omega_{IAP}^{Rand}(k_{LO}, k_{RO}, k_V, k_{LH}, k_{RH}, k) = 3^{k-1} + \sum_{\mu_{IAP}^{Rand}=k}^{\alpha k-1} \left(\sum_{C_1, C_2} \binom{\mu_{IAP}^{Rand}}{k_{LO}, k_{RO}, k_V, k_{LH}, k_{RH}} \right)$$

where $C_1 \stackrel{\text{def}}{=} k_{LO} + k_{RO} + k_V = k - 1$ and $C_2 \stackrel{\text{def}}{=} k_{LH} + k_{RH} = \mu_{IAP}^{Rand} - (k - 1)$.

Proof: We demonstrated in Theorem 1 that the total number of intruder's abstract paths, which have only left-oblique, right-oblique, and/or vertical line-segments, is 3^{k-1} . The length of each of these paths is $k - 1$. The first part of $\Omega_{IAP}^{Rand}(k_{LO}, k_{RO}, k_V, k_{LH}, k_{RH}, k)$, namely 3^{k-1} , accounts for those paths having such a length. However, the second part of $\Omega_{IAP}^{Rand}(k_{LO}, k_{RO}, k_V, k_{LH}, k_{RH}, k)$, namely $\sum_{\mu_{IAP}^{Rand}=k}^{\alpha k-1} \left(\sum_{C_1, C_2} \binom{\mu_{IAP}^{Rand}}{k_{LO}, k_{RO}, k_V, k_{LH}, k_{RH}} \right)$, accounts for those paths whose length μ_{IAP}^{Rand} is larger than $k - 1$. Each of such paths should contain $k - 1$ left-oblique, right-oblique, and/or vertical line-segments (*condition* C_1), and the other remaining $\mu_{IAP}^{Rand} - (k - 1)$ edges have to be left-horizontal and/or right-horizontal line-segments (*condition* C_2). The inner summation of this second part is similar to the one given in Theorem 1. It computes the number of intruder's abstract paths whose length is μ_{IAP}^{Rand} and each of which has k_{LO} left-oblique line-segments, k_{RO} right-oblique line-segments, and/or k_V vertical line-segments, and k_{LH} left-horizontal line-segments and/or k_{RH} right-horizontal line-segments, subject to those two conditions, *i.e.*, C_1 and C_2 . The outer summation of this second part accounts for all paths whose length varies between k and $\alpha k - 1$, which corresponds to the longest intruder's abstract path. ■

6 Performance Evaluation

In this section, we specify the simulation setup. Then, we present some simulation results using a high-level simulator written in C.

6.1 Simulation Setup

We consider a rectangular belt of the following dimensions: Its width w takes on its values in the set $\{50\text{m}, 60\text{m}, 70\text{m}, 80\text{m}, 90\text{m}, 100\text{m}\}$, and its length $l = 3000\text{m}$. We assume that the sensors are densely and randomly deployed in this rectangular belt, and that their sensing and communication ranges are equal to 5m and 10m, respectively. The number of deployed sensors is set to 5000. Notice that the number of required sensors for deterministic sensor deployment based on square lattice (see Theorem 5) and hexagonal lattice (see Theorem 6) for $w = 100\text{m}$ are respectively given by $n_{SL} = 3000 < 5000$, and $n_{HL} = 3305 < 5000$. This shows that the sensors are densely deployed. In fact, the number of required sensors is much smaller for the other smaller values of w , *i.e.*, $\{50\text{m}, 60\text{m}, 70\text{m}, 80\text{m}, 90\text{m}\}$. Also, we assume that an intruder moves across the rectangular belt from top to bottom. That is, if $(x(t), y(t))$ is the position of an intruder at time t , $(x(t + 1), y(t + 1))$ is its position at time $t + 1$ such that the following conditions are met:

$$0 \leq x(t), x(t + 1) \leq l = 3000$$

$$0 \leq y(t + 1) \leq y(t) \leq w$$

There is no relationship between the x -coordinates of the intruder's location at times t (*i.e.*, $x(t)$) and $t + 1$ (*i.e.*, $x(t + 1)$). However, the y -coordinates of the intruder's location should satisfy $y(t + 1) \leq y(t)$ so an intruder makes progressive movement as they cross the rectangular sensor belt.

6.2 Simulation Results

Figures 12 and 13 are for square lattice-based analysis, while Figures 14 and 15 are for hexagonal lattice-based analysis. That

is, for random sensor deployment, we want to select the sensors whose locations correspond or are close to their counterparts in square and hexagonal lattices, respectively, so the rectangular sensor belt is k -covered. Figures 12 and 13 show that the number of selected sensors to generate square lattice and hexagonal lattice, respectively, is higher than the number of sensors needed for square lattice-based and hexagonal lattice-based deterministic sensor deployment, respectively. This is mainly due to randomness. It is not always possible to extract a square lattice or hexagonal lattice from randomly deployed sensors. Also, the number of sensors needed to generate a square lattice is smaller than its counterpart to produce a hexagonal lattice. Figures 14 and 15 show that rate of intruder detection associated with the generated hexagonal lattice is higher than its counterpart corresponding to the produced square lattice. Indeed, a denser sensor deployment improves the percentage of detection of intruder while crossing the k -covered sensor belt region. Moreover, as w increases, k increases (*i.e.*, k is linearly proportional to w), the rate of intruder detection increases. As discussed earlier in Section 1, the presence of multiple layers (*i.e.*, layered protection system) makes the likelihood of an intruder being caught (or detected) high.

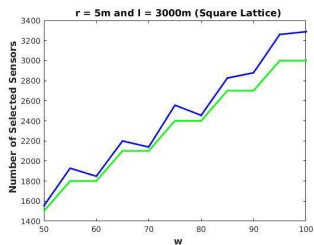


Figure 12. Square Lattice

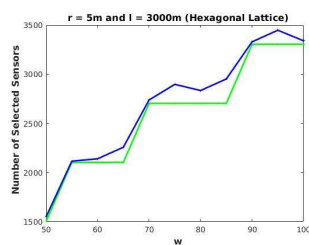


Figure 13. Hexagonal Lattice

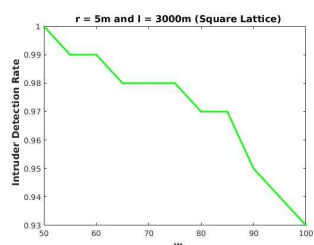


Figure 14. Square Lattice

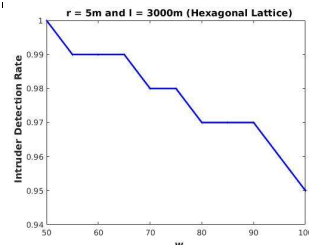


Figure 15. Hexagonal Lattice

7 Conclusion

Providing perimeter intrusion detection to a critical area is a requirement to achieve physical security objective. Among others, an international border is one instance of the above-mentioned physical security problem. We found that wireless sensor networks can be deployed to build a belt of sensors (or barrier) around a protected area to detect and prevent any intruder crossing it. In this paper, we attempted to solve the problem of k -barrier coverage, where every path crossing this barrier intersects with at least k sensors. First, we considered two deterministic lattice-based sensor deployment strategies: Square lattice and hexagonal lattice. Second, we represented the walk of an intruder across this barrier by an abstract path, which includes progressive moves, each of which having the form of left-oblique, right-oblique, or vertical line segment. Then, we derived several theoretical results, such as the total

number of intruder's abstract paths along with their polynomial representation, the total number of sensors, and the intruder's abstract path observability for square and hexagonal lattices based k -barrier coverage. We proposed a generalization of these results by considering a random intruder's trajectory across a k -barrier covered sensor belt, which is characterized by a sequence of left-horizontal, right-horizontal, left-oblique, right-oblique, and/or vertical (for square lattice only) line segments.

Our future work is two-fold. First, we plan to extend our analysis to heterogeneous sensors. Second, we want to consider the case of three-dimensional WSNs, which model more accurately several real-world physical security scenarios

8 References

- [1] H. M. Ammari, "Investigating the energy sink-hole problem in connected k -covered wireless sensor networks," *IEEE TC*, 63(11), pp. 2729-2742, Nov. 2014.
- [2] F. Aurenhammer, "Voronoi diagrams — A survey of a fundamental geometric data structure," *ACM Computing Surveys*, 23(3), pp. 345-405, Sep. 1991.
- [3] A. Chen, S. Kumar, and T. H. Lai, "Local barrier coverage in wireless sensor networks," *IEEE TMC*, 9(4), pp. 491-504, 2010.
- [4] S. He, X. Gong, J. Zhang, J. Chen, and Y. Sun, "Curve-based deployment for barrier coverage in wireless sensor networks," *IEEE TWC*, 13(2), pp. 724-735, Feb. 2014.
- [5] S. He, X. Gong, J. Zhang, J. Chen, and Y. Sun, "Barrier coverage in wireless sensor networks: From lined-based to curve-based deployment," *Proc. IEEE INFOCOM*, pp. 470-474, 2013.
- [6] D. Kim, H. Kim, D. Li, S.-S. Kwon, A. O. Tokuta, and J. A. Cobb, "Maximum lifetime dependable barrier-coverage in wireless sensor networks," *Elsevier Ad Hoc Networks*, 36, pp. 296-307, Jan. 2016.
- [7] H. Kim, J. A. Cobb, and J. Ben-Othman, "Maximizing the lifetime of reinforced barriers in wireless sensor networks," *Wiley Concurrency and computation: Practice and experience*, 2016.
- [8] S. Kumar, T. H. Lai, and A. Arora, "Barrier coverage with wireless sensors," *Proc. ACM MobiCom*, 2005.
- [9] S. Kumar, T. H. Lai, M. E. Posner, and P. Sinha, "Maximizing the lifetime of a barrier of wireless sensors," *IEEE TMC*, 9(8), pp. 116-1172, Apr. 2010.
- [10] B. Liu, O. Dousse, J. Wang, and A. Saipulla, "Strong barrier coverage of wireless sensor networks," *Proc. ACM MobiHoc*, pp. 411-420, 2008.
- [11] S. Megerian, F. Koushanfar, M. Potkonjak, and M. Srivastava, "Worst and best-case coverage in sensor networks," *IEEE TMC*, 4(1), pp. 84-92, 2005.
- [12] S. Megerian, F. Koushanfar, M. Potkonjak, and M. Srivastava, "Coverage problems in wireless ad-hoc sensor networks," *Proc. IEEE Infocom*, pp. 1380-1387, 2001.
- [13] A. Saipulla, C. Westphal, B. Liu, and J. Wang, "Barrier coverage with line-based deployed mobile sensors," *Elsevier Ad Hoc Networks*, 11, pp. 1381-1391, 2013.
- [14] A. Saipulla, B. Liu, G. Xing, X. Fu, and J. Wang, "Barrier coverage with sensors of limited mobility," *Proc. ACM MobiHoc*, 2010.
- [15] B. Wang, "Coverage problems in sensor networks: A survey," *ACM Computing Surveys*, 43(4), Article 32, pp. 32:1-32:53, Oct. 2011.
- [16] Z. Wang, J. Liao, Q. Cao, H. Qi, and Z. Wang, "Achieving k -barrier coverage in hybrid directional sensor networks," *IEEE TMC*, 13(7), pp. 1443-1455, Jul. 2014.
- [17] G. Yang and D. Qiao, "Barrier information coverage with wireless sensors," *Proc. IEEE INFOCOM*, 2009.
- [18] H. Yang, D. Li, Q. Zhu, W. Chen, and Y. Hong, "Minimum energy cost k -barrier coverage in wireless sensor networks," *WASA*, LNCS 6221, pp. 80-89, 2010.
- [19] F. Ye, G. Zhong, J. Cheng, S. Lu, and L. Zhang, "PEAS: A robust energy conserving protocol for long-lived sensor networks," *Proc. ICDCS*, 2003.